British Journal of Pharmacology

British Journal of Pharmacology (2017) **174** 893–908 893

RESEARCH PAPER

Inhibition of 6-phosphofructo-2-kinase suppresses fibroblast-like synoviocytes-mediated synovial inflammation and joint destruction in rheumatoid arthritis

Correspondence Hanshi Xu, Department of Rheumatology, The First Affiliated Hospital, Sun Yat-sen University, No.58 Zhongshan Road 2, Guangzhou, Guangdong 510080, China. E-mail: xuhanshi@hotmail.com

Received 4 July 2016; **Revised** 15 February 2017; **Accepted** 17 February 2017

Yaoyao Zou*, Shan Zeng*, Mingcheng Huang*, Qian Qiu, Youjun Xiao, Maohua Shi, Zhongping Zhan, Liuqin Liang, Xiuyan Yang and Hanshi Xu

Department of Rheumatology, The First Affiliated Hospital, Sun Yat-sen University, Guangzhou, Guangdong, China

*Y Zou, S Zeng and M Huang contributed equally to this work.

BACKGROUND AND PURPOSE

Abnormal glycolytic metabolism contributes to joint inflammation in rheumatoid arthritis (RA). The aims of this study were to investigate the role of 6-phosphofructo-2-kinase/fructose-2,6-bisphosphatase 3 (PFKFB3), a bifunctional enzyme that controls the glycolytic rate, in regulating fibroblast-like synoviocyte (FLS)-mediated synovial inflammation and invasiveness in RA.

EXPERIMENTAL APPROACH

A specific inhibitor of PFKFB3, PFK15, and siRNA were used to evaluate the role of PFKFB3. Protein expression was measured by Western blotting or immunofluorescence staining. The expression of cytokines was determined by quantitative real-time PCR. Migration and invasion were measured using a Boyden chamber assay. A mouse model of collagen-induced arthritis (CIA) was used to evaluate the *in vivo* effect of PFK15.

KEY RESULTS

PFKFB3 expression was increased in the synovial tissue and FLSs from RA patients compared with osteoarthritis patients. PFKFB3 inhibition decreased the expression of IL-8, IL-6, CCL-2 and CXCL-10 and the proliferation, migration and invasion of RA FLSs. PFK15 suppressed TNF-α-induced activation of NF-κB and p38, JNK and ERK MAPK signals in RA FLSs. PFK15 treatment also suppressed glucose uptake and lactate secretion. Lactate reversed the inhibitory effect of PFK15 or PFKFB3 siRNA on cytokine expression and migration of RA FLSs. Lactate was also involved in PFKFB3-mediated activation of NF-κB and MAPKs. Intraperitoneal injection of PFK15 in mice with CIA attenuated joint inflammation.

CONCLUSION AND IMPLICATIONS

Elevated PFKFB3 expression might contribute to synovial inflammation and aggressive behaviours of RA FLSs, suggesting a novel strategy of targeting PFKFB3 to prevent synovial inflammation and joint destruction in RA.

Abbreviations

CIA, collagen-induced arthritis; EdU, 5-ethynyl-2´-deoxyuridine; F2,6BP, fructose 2,6-bisphosphate; FLS, fibroblast-like synoviocytes; IF, immunofluorescence; IKKβ, inhibitor of NF-κB kinase β; OA, osteoarthritis; PFKFB, 6-phosphofructo-2-kinase/fructose-2,6-bisphosphatase; RA, rheumatoid arthritis

DOI:10.1111/bph.13762

Tables of Links

TARGETS
Enzymes
IKK-β
p38-α (MAPK14)
JNK1 (MAPK8)
ERK

LIGANDS
L-lactic acid
TNF-α
IL-6
IL-8 (CXCL8)

These Tables list key protein targets and ligands in this article that are hyperlinked to corresponding entries in http://www.guidetopharmacology.org, the common portal for data from the IUPHAR/BPS Guide to PHARMACOLOGY (Southan *et al.*, 2016), and are permanently archived in the Concise Guide to PHARMACOLOGY 2015/16 (Alexander *et al.*, 2015).

Introduction

Rheumatoid arthritis (RA) is a chronic inflammatory disease characterized by chronic synovial inflammation and progressive joint destruction. Fibroblast-like synoviocytes (FLSs) in the synovial intimal lining play a key role in the initiation and development of synovial inflammation and joint destruction associated with RA. Stable-activated RA FLSs exhibit an abnormal capacity for migration, invasion and secretion of proinflammatory cytokines and chemokines (Choy, 2012; Turner and Filer, 2015). Growing evidence suggests that targeting FLS-mediated synovial inflammation and invasion may be a new therapeutic avenue for RA (Bottini and Firestein, 2013).

Glucose metabolism provides energy for physical activity and also modulates many physiological processes through the formation of complex signalling networks with metabolic substrates. Targeting glucose metabolism reprogramming is considered a promising strategy for the development of new cancer therapeutics (Lunt and Vander Heiden, 2011; Schulze and Harris, 2012). A recent study showed that increased glycolytic metabolism in RA FLSs contributes to synovial inflammation and joint damage, suggesting that glycolytic suppression might be an effective therapeutic strategy for inflammatory arthritis (Garcia-Carbonell *et al.*, 2016).

A critical event in the glycolytic breakdown of glucose is the phosphorylation of fructose 6-phosphate (F6P) to fructose 1,6 bisphosphate (F1,6P2) by 6-phosphofructo-1-kinase (PFK1). Fructose 2,6-bisphosphate (F2,6BP) is the most important downstream metabolite in the control of PFK1 (Van Schaftingen *et al.*, 1980). The bifunctional 6-phosphofructo-2-kinase/fructose-2,6-bisphosphatase (PFKFB) enzymes both catalyse the production and degradation of F2,6BP through kinase and phosphatase functions (Okar *et al.*, 2001; Rider *et al.*, 2004). The PFKFB family consists of four isoenzymes, PFKFB1–4. Of all PFKFB members, PFKFB3 has much higher (740-fold) kinase than bisphosphatase activity, enhancing the production of F2,6P2 and thus critically controlling the glycolytic rate under normal and pathophysiological conditions (Van Schaftingen *et al.*, 1982; Chesney *et al.*, 2005; Clem *et al.*, 2008). PFKFB3 inhibition decreases the proliferation and activation of anti-CD3/CD28-induced human T cells (Telang *et al.*, 2012). A low MW antagonist of PFKFB3, 3-(3-pyridinyl)-1-(4-pyridinyl)-2-propen-1-one (3PO), reduces glycolytic flux and tumour growth (Clem *et al.*, 2008). However, the role of PFKFB3 in the pathogenesis of RA remains poorly defined. In this study, we utilized a potent and selective PFKFB3 inhibitor, PFK15 (Clem *et al.*, 2013), to investigate the contribution of PFKFB3 to synovial inflammation and joint destruction in RA.

Methods

Preparation of synovial tissue and fibroblast-like synoviocytes (FLSs)

The human study protocol was approved by the Medical Ethical Committee of the First Affiliated Hospital at Sun Yat-sen University [protocol number (2014)C-059] and was conducted according to the recommendations of the Declaration of Helsinki. All patients provided informed consent to participate in the study. RA was diagnosed according to the 1987 revised criteria of the American College of Rheumatology (Arnett *et al.*, 1988).

Synovial tissue samples were obtained from 12 patients with RA (10 women and two men, aged 45–62 years) and nine patients with osteoarthritis (OA) (seven women and two men, aged 52–61 years) who were undergoing synovectomy or joint replacement.

The synovial tissue from patients was cut into small pieces and digested with collagenase I in DMEM/F12 medium to isolate synoviocytes. The cells were grown in DMEM/F12 medium containing 10% FBS, 100 $U \cdot mL^{-1}$ penicillin and 100 $\mu g \cdot mL^{-1}$ streptomycin in a humidified incubator at 37°C under 5% CO_2. The cells were used from passage 3 to 5, during which time they were a homogeneous population of cells (<1% CD11b-positive, <1% phagocytic and <1% FcgRII and FcgRIII receptor-positive) and were characterized by vimentin and cadherin-11, a FLS-specific marker (Chang *et al.*, 2010). Cell viability was measured using an MTT assay, as previously described (Xu *et al.*, 2007).

PFKFB3 siRNA transfection

PFKFB3 siRNA, non-silencing control siRNA and GAPDH siRNA were obtained from Guangzhou RiboBio Co., Ltd (Guangzhou, China). The sequences of PFKFB3 siRNA oligonucleotides are shown in Table S1 (Supporting Information). RA FLSs were cultured in 12-well plates. A transfection mixture of 100 nM siRNA and 10 $mg{\cdot}mL^{-1}$ lipofectin in serum-free medium was added to medium-aspirated FLSs for 4 h. The FLSs were then incubated with complete DMEM/F12 containing 10% FBS for 48 h before the experiments. At the end of the culture, the effect of the siRNA on PFKFB3 expression was analysed using quantitative real-time PCR and Western blot analysis.

Western blot analysis

Western blot analysis was performed as described previously (Xu *et al.*, 2007). The protein concentrations were measured using a BCA protein assay (Pierce, Rockford, IL, USA). Primary antibodies were diluted 1:1000 for PFKFB3 and 1:500 for phospho-IKK, IKK, phospho-IκBα and IκBα. Densitometry was performed using an AlphaEaseFc (Fluorchem8900) system.

Cell migration and invasion assay

The FLS chemotaxis assay was performed using Boyden chambers with a 6.5-mm-diameter filter and 8.0 μm pore size (Transwell; Corning Inc., Corning, NY, USA). Briefly, FLSs (at a final concentration of 6×10^4 $cells{\cdot}mL^{-1}$) were suspended in serum-free DMEM in the upper wells. TNF-α ($10\ ng{\cdot}mL^{-1}$) was used as a chemoattractant. The chamber was incubated at 37°C under 5% CO_2 for 8 h. After incubation, the non-migrating cells were removed from the upper surface of the filter using a cotton swab. The filters were fixed in methanol for 15 min and stained with 0.1% crystal violet for 15 min. Chemotaxis was quantified by counting the stained cells that migrated to the lower side of the filter using an optical microscope. The stained cells were counted as the mean number of cells per 10 random fields for each assay. For the invasion assay, similar experiments were performed using inserts coated with a Matrigel basement membrane matrix (BD Biosciences, Oxford, UK).

Wounding migration

Cultures of RA FLSs were wounded with 1 mL micropipette tips and then washed three times with starving medium to remove unattached cells. The remaining cells were treated with or without PFK15. After 24 h of incubation, migration was quantified by counting the cells that had moved beyond a reference line.

Immunohistochemistry

For immunohistochemistry, synovial tissue sections were deparaffinized followed by incubation with 5% serum in PBS for 2 h to block non-specific binding and incubation with 3% H_2O_2 for 10 min to block endogenous peroxidase activity. The expression of PFKFB3 or IL-6 was determined by staining with polyclonal rabbit anti-human PFKFB3 or anti-mouse IL-6 antibody overnight at 4°C. Irrelevant isotype-matched antibodies were used as controls. Polyclonal goat anti-rabbit antibodies labelled with HRP were used as secondary antibodies for 1 h at room temperature. Results were revealed using diaminobenzidine.

Immunofluorescence (IF) staining

FLSs were cultured on coverslips under identical conditions to those described above. The cells were fixed with acetone at −20°C and permeabilized with 0.1% Triton X-100 in PBS for 5 min at room temperature. The cells were incubated with primary antibodies (diluted 1:100 for anti-p65 antibody, diluted 1:200 for PFKFB3 antibodies) for 1 h at room temperature and then incubated with fluorescein isothiocyanate-conjugated secondary antibody (Santa Cruz Biotechnology). After washing in PBS, the cells were incubated for 3 min with 0.25 $mg{\cdot}mL^{-1}$ of DAPI. The coverslips were mounted on glass slides with antifade mounting medium and examined using a confocal fluorescence microscope (LSM510; Zeiss, Wetzlar, Germany).

Quantitative real-time PCR

Total RNA from RA FLSs was prepared using the Takara PrimeScript® RT reagent kit according to the manufacturer's protocol. Quantitative real-time PCR was performed using the Bio-Rad CFX96 system. The primers employed for real-time PCR are listed in Table 1. To quantify the relative expression of each gene, Ct values were normalized to the endogenous reference (△Ct = Ct target-Ct 18S rRNA) and compared with a calibrator using the △△Ct method (△△Ct = △Ct sample-△Ct calibrator). All experiments were performed in triplicate.

FLS proliferation assays

RA FLSs were cultured for 24 h at a density of 1×10^4 cells per well in 96-well plates in serum-free medium. After starving,

Table 1

The sequences of RT-PCR primers

	Sequences	
CCL2	Forward	CAGCCAGATGCAATCAATGCC
	Reverse	TGGAATCCTGAACCCACTTCT
IL-6	Forward	ACTCACCTCTTCAGAACGAATTG
	Reverse	CCATCTTTGGAAGGTTCAGGTTG
IL-8	Forward	ACTGAGAGTGATTGAGAGTGGAC
	Reverse	AACCCTCTGCACCCAGTTTTC
CXCL10	Forward	GTGGCATTCAAGGAGTACCTC
	Reverse	TGATGGCCTTCGATTCTGGATT
PFKFB1	Forward	AGAAGGGGCTCATCCATACCC
	Reverse	CTCTCGTCGATACTGGCCTAA
PFKFB2	Forward	TGGGCCTCCTACATGACCAA
	Reverse	CAGTTGAGGTAGCGTGTTAGTTT
PFKFB3	Forward	AGCCCGGATTACAAAGACTGC
	Reverse	GGTAGCTGGCTTCATAGCAAC
PFKFB4	Forward	TCCCCACGGGAATTGACAC
	Reverse	GGGCACACCAATCCAGTTCA
GAPDH	Forward	GCACCGTCAAGGCTGAGAAC
	Reverse	TGGTGAAGACGCCAGTGGA

the cells were incubated with various concentrations of PFK15 for 48 h and then incubated with 5-ethynyl-2´-deoxyuridine EdU (50 μM) for 8 h. The Cell-Light EdU DNA Cell Proliferation Kit was used to measure FLS proliferation according to the manufacturer's instructions.

Glucose uptake measurements

Glucose uptake was measured using a glucose uptake assay kit (colorimetric, Abcam) according to the manufacturer's instructions.

Lactate measurements

Lactate levels in the medium were detected using a lactate oxidase-based assay at 540 nm. All experiments were performed in triplicate.

Fructose-2,6-bisphosphate (F2,6BP) assay

RA FLSs (1×10^6) were harvested and centrifuged at 200 g. The pellets were dissolved in 50 mM Tris acetate (pH 8.0) and 0.1 M NaOH. Intracellular F2,6BP levels were measured using a previously described method (Van Schaftingen *et al.,* 1982). The F2,6BP concentration was normalized to total cellular protein.

Administration of PFK15 in mice with collagen-induced arthritis (CIA)

All animal care and experimental procedures were approved by the Animal Care and Ethics Committee of the First Affiliated Hospital at Sun Yat-sen University [protocol number (2014)A-019] and complied with the Guide for the Care and Use of Laboratory Animals, which was published by the US National Institutes of Health. Animal studies are reported in compliance with the ARRIVE guidelines (Kilkenny *et al*., 2010; McGrath and Lilley, 2015).

Mice (n = 22) were injected intradermally at the base of the tail with 200 μg of bovine type II collagen (Sigma, St Louis, MO, USA) diluted in acetic acid and emulsified at a 1:1 ratio (vol/vol) in Freund's complete adjuvant. Three weeks after primary immunization, the mice were boosted by i.p. injection of bovine type II collagen emulsified at a 1:1 ratio (vol/vol) in incomplete Freund's adjuvant. Disease onset characterized by erythema and/or paw swelling was observed from day 32 to 41 after the first immunization. The animals were treated randomly via i.p. injection of PFK15 (25 $mg \cdot kg^{-1}$, every other day, n = 8) or DMSO (vehicle, n = 8) for a total of 14 days, initiated on the day of arthritis onset (day 0). The mice were monitored daily for signs of arthritis, and arthritis severity was scored on a scale from 0 to 3, as described previously (Leung *et al.,* 2003). The arthritic score was determined for all four paws of the mice. The ankle diameter was determined using a 0.01 mm precision Vernier calliper. All mice were anaesthetised with 110 $mg \cdot kg^{-1}$ ketamine and 4.8 $mg \cdot kg^{-1}$ xylazine, and their hind limbs were removed and fixed in 10% neutral-buffered formalin. The tissue was decalcified in 8% formic acid and embedded in paraffin. Sections (3 μm) were stained with haematoxylin and eosin (H&E). An inflammation score was obtained using the scoring system described previously (Leung *et al.,* 2003).

To determine the serum level of IL-6, serum samples were collected from mice. The levels of IL-6 were measured using an ELISA kit according to the manufacturer's instructions (R&D Systems, USA).

To evaluate the toxic effect of PFK15 on mice with CIA, biochemical analyses of serum samples were determined by a colorimetric enzymic method using spectrophotometry. The enzymic activities of aspartate aminotransferase (AST) and alanine aminotransferase (ALT) were measured to assess changes in liver function. Serum creatinine was used as a marker of renal function. Histopathology of the liver and kidney was also observed by staining with H&E.

Data and statistical analysis

The data and statistical analysis comply with the recommendations on experimental design and analysis in pharmacology (Curtis *et al.,* 2015). Data are expressed as the means ± SEM. Presented values were derived from at least five independent experiments for the *in vitro* experiments. The experimental procedures or treatment and data analyses were performed with blinding. To reduce baseline variability between independent experiments, normalization was performed for the quantitative analysis of immunoblots, glucose uptake and mRNA expression. The data were normalized as the fold over the mean of the control. Two groups were compared by Student's t-test. Three or more different groups were evaluated by one-way ANOVA. ; Only if F achieved $P < 0.05$, and there was no significant variance in homogeneity, we applied two *post hoc* tests; Dunnett's *post hoc* test when comparing each group with the control or the Sidak *post hoc* test if a multiple group comparison was necessary. A non-parametric analysis was performed to analyse the normalization of the generated data. Non-parametric data were analysed with the Kruskal–Wallis test or Wilcoxon two-sample test. A P-value ≤0.05 was considered significant. Statistical analyses of the data were performed using SPSS 13.0 software.

Materials

TNF-α was obtained from R&D Systems (R&D Systems, Minneapolis, MN). PFK15 was obtained from Selleck Chemicals. DMEM/Ham's F12 (F12), FBS, antibiotics, trypsin–EDTA, PBS and other reagents for cell culture were purchased from Invitrogen (Carlsbad, CA, USA). Collagenase and β-actin antibody were purchased from Sigma (St. Louis, MO, USA). p65, IKK-β, phospho-IKK, IκBα, phospho-IκBα, p38, phospho-p38, JNK, phospho-JNK, ERK and phospho-ERK antibodies were purchased from Santa Cruz Biotechnology (Santa Cruz, CA, USA).

Results

PFKFB3 expression is increased in FLSs and synovial tissue from RA patients

First, we determined the expression patterns of PFKFB isoenzymes in FLSs. Analysis of FLSs by qRT-PCR revealed no expression of PFKFB1 mRNA. However, PFKFB2, PFKFB3 and PFKFB4 were transcribed in FLSs from RA and OA patients. We further observed that only PFKFB3 expression was increased in RA FLSs compared with the expression levels in OA FLSs (Figure 1A).

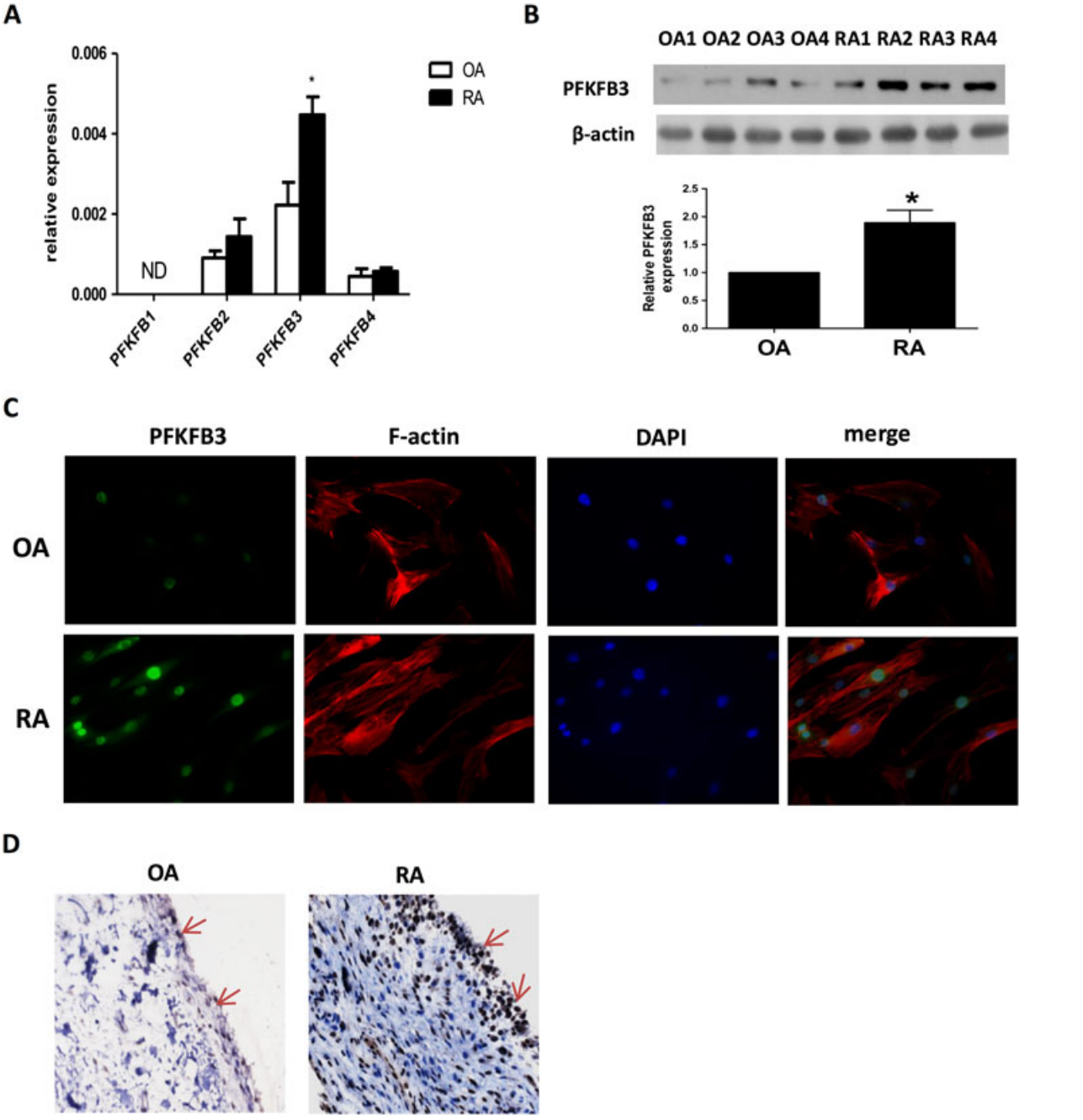

Figure 1

Expression patterns of PFKFB3 in FLSs and synovial tissues from patients with RA. (A) PFKFB isoenzyme mRNA expression in FLSs. PFKFB mRNA expression was determined by qRT-PCR analysis. The data represent the means ± SEM from FLSs obtained from the synovial tissues of patients with RA ($n = 12$) and OA ($n = 9$). (B) Representative images of Western blot analyses showing the expression of PFKFB3 in RA FLSs ($n = 12$) and OA FLSs ($n = 9$). The data represent the means ± SEM of the densitometric quantification (lower panel). (C) The location of PFKFB3 in RA FLSs. Immunofluorescence staining was used to determine the expression of PFKFB3. The nuclei were stained with DAPI, and F-actin was stained with phalloidin. Representative laser confocal microscopy images show the staining of PFKFB3 from patients with RA ($n = 6$) and OA ($n = 5$). Original magnification 400×. (D) PFKFB3 expression in synovial tissues. Representative images of immunohistochemical staining of tissues from patients with RA ($n = 6$) and OA ($n = 3$). Arrows indicate PFKFB3 staining. Original magnification 100×. *$P < 0.05$, significantly different from OA.

Next, we evaluated the protein expression of PFKFB3 in FLSs. Western blot analysis revealed that PFKFB3 expression was increased in RA compared with that in OA patients (Figure 1B). Using IF analysis, PFKFB3 protein was localized predominantly in the nucleus (Figure 1C). Moreover, PFKFB3 expression was prominent in synovial tissues from RA patients and mostly localized in the synovial lining and sublining cells, whereas the expression was much less prominent in synovial tissues from OA patients (Figure 1D).

PFKFB3 inhibition decreases the expression of proinflammatory cytokines and chemokines in RA FLS

PFK15 is a potent and selective inhibitor of PFKFB3 (Clem *et al.*, 2013). To evaluate the role of PFKFB3 in the pathogenesis of RA, RA FLSs were treated with various concentration of PFK15. As shown in Figure 2A, TNFα-induced expression of IL-6, IL-8, CCL-2 and CXCL-10 was reduced by treatment with PFK15 at concentrations ranging from 0.5 to 5.0 μM. The viability of RA FLSs was measured by the MTT assay to evaluate the toxic effect of PFK15 on RA FLSs. Up to 10 μM, this compound did not reduce cell

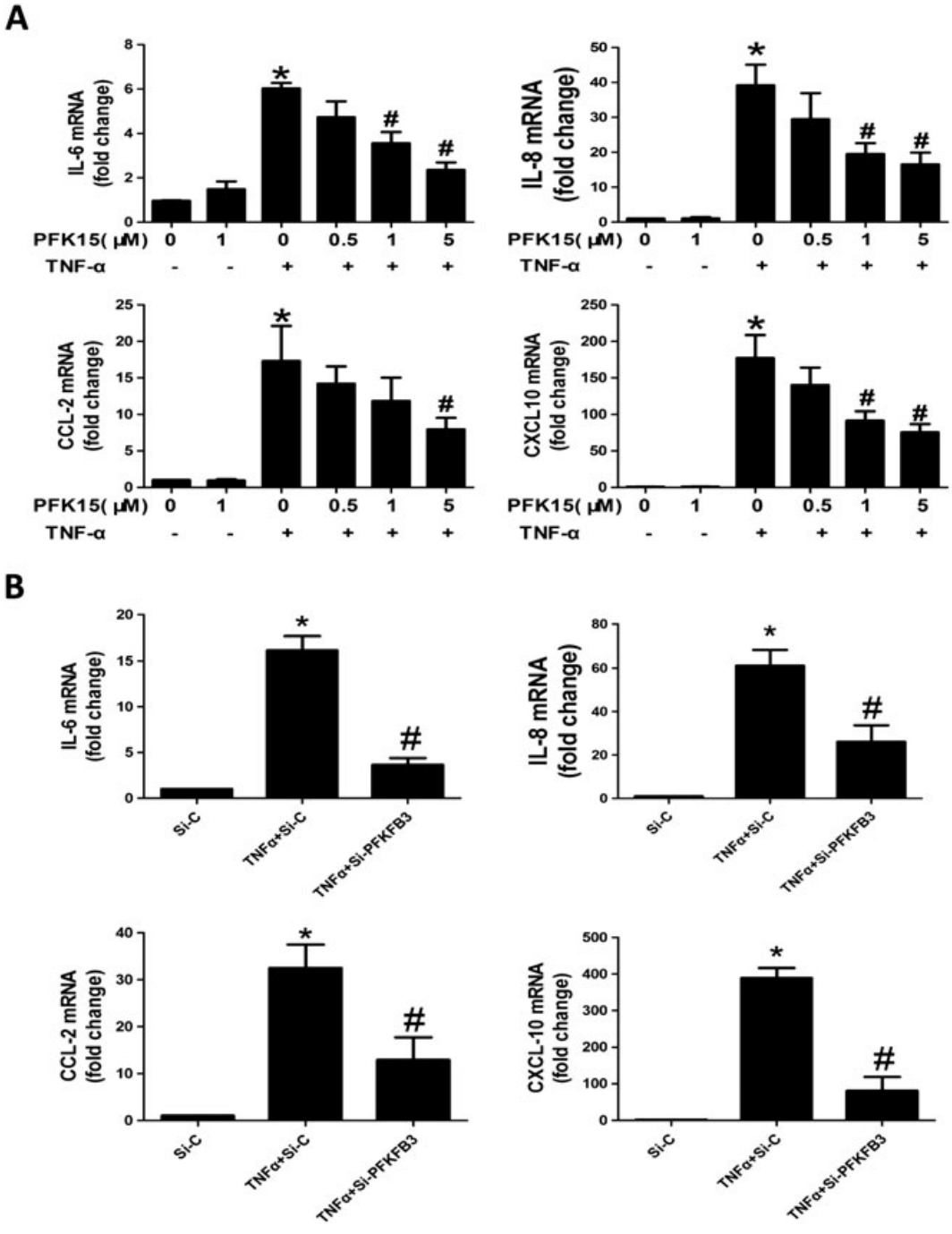

Figure 2

Effects of PFKFB3 inhibition on the expression of proinflammatory cytokines and chemokines in RA FLSs. RA FLSs were pretreated with DMSO (as the control) or various concentrations of a specific PFKFB3 inhibitor, PFK15, for 4 h (A) or were transfected with specific PFKFB3 siRNA (SiPFKFB3) or control siRNA (SiC) and then stimulated with or without TNF-α (10 ng·mL^{-1}) for 24 h (B). The expression of IL-6, IL-8, CCL-2 and CXCL-10 was measured by real-time qPCR. The data are representative of independent experiments (means ± SEM) from 10 RA patients. *$P < 0.05$, significantly different from control or SiC; $^{\#}P < 0.05$, significantly different from treatment with TNF-α alone.

viability (data not shown), which indicated that the observed inhibitory effects were not caused by cytotoxic effects.

To rule out a non-specific effect of the low MW inhibitor, we utilized RNA interference to selectively reduce PFKFB3 expression. We constructed three different sequences of siRNA oligonucleotides for PFKFB3. Transfection with all three siRNA oligonucleotides down-regulated endogenous PFKFB3 protein expression; however, the inhibitory effect of siRNA-3 was the most prominent (Supporting Information Fig. S1 in the supplemental data). Therefore, PFKFB3 siRNA-3 (Si-PFKFB3) was used for further experiments.

After 72 h of transfection with PFKFB3 siRNA or control siRNA, the cells were treated with TNF-α for 24 h. Transfection with siRNA directed against PFKFB3 decreased TNF-α-induced cytokine expression compared with that in cells that received the control siRNA treatment (Figure 2B) and further confirmed our results obtained with PFK15.

PFKFB3 inhibition impairs the migration, invasion and proliferation of RA FLS

To examine the role of PFKFB3 in the migration of RA FLSs, chemotaxis of FLSs was evaluated using a Transwell chamber assay. As shown in Figure 3A, treatment with PFK15 decreased the chemotactic migration of RA FLSs. In addition, treatment with PFKFB3 siRNA resulted in a reduction in the migration of RA FLSs compared with that seen in cells transfected with the non-silencing control vector (Figure 3B). Furthermore, a monolayer wound-healing assay was used to evaluate the role of PFKFB3 in cell migration. Wound closing was significantly slowed in cultures of RA FLSs treated with PFK15 or PFKFB3 siRNA (Figure 3C).

The *in vitro* invasion potential of RA FLSs is highly correlated with the rate of joint destruction in RA patients (Tolboom *et al.,* 2005). To evaluate the role of PFKFB3 in the invasive behaviour of RA FLSs, a thin layer of reconstituted extracellular matrix (Matrigel) was used to measure the *in vitro* invasion of RA FLSs. We found that PFK15 treatment suppressed Matrigel invasion of RA FLSs (Figure 3D and E).

To determine if PFKFB3 could regulate the proliferation of RA FLSs, the cells were treated with EdU (50 μM). As shown in Figure 3F and G, treatment with PFK15 or PFKFB3 siRNA decreased the proliferation of RA FLSs.

PFKFB3 inhibition reduces the activation of NF-κB and MAPK in RA FLS

To determine whether PFKFB3 inhibition affects activation of NF-κB, we first evaluated the effect of PFK15 on the nuclear translocation of p65, a key step in the control of NF-κB activation. As shown in Figure 4A, we observed a reduction in p65 nuclear accumulation in RA FLSs treated with PFK15, compared with that in cells treated with TNF-α alone. Furthermore, we observed a decrease in phosphorylated IKKβ following treatment with PFK15 in TNF-α-stimulated RA FLSs (Figure 4B). Consistent with the decreased IKK activity, PFK15 treatment also suppressed the TNF-α-induced phosphorylation and degradation of IκBα (Figure 4B).

Next, we evaluated the role of PFKFB3 in regulating the activation of MAPK pathways, important signals involved in modulating synovial inflammation and joint destruction in RA. We observed that phosphorylation of p38, JNK and ERK was robustly induced after treatment with TNF-α, but PFK15 treatment suppressed TNF-α-induced phosphorylation of p38, JNK and ERK (Figure 4C).

PFKFB3 inhibition reduces glucose uptake and intracellular levels of fructose-2,6-bisphosphate (F2,6BP) by RA FLS

To investigate whether PFKFB3 inhibition could affect glycolysis in RA FLSs, we assessed the effects of PFK15 or PFKFB3 siRNA on glucose uptake and secretion of lactate. As shown in Figure 5A, glucose uptake was markedly increased in TNF-α-induced RA FLSs. Treatment with PFK15 or PFKFB3 siRNA decreased both basal and TNF-α-induced, glucose uptake. Similarly, intracellular levels of F2,6BP were also increased after stimulation with TNF-α, and this increase was suppressed by treatment with PFK15 (Figure 5B).

Lactate is involved in PFKFB3-mediated inflammation and RA FLS migration

To determine the role of lactate in PFKFB3-associated synovial inflammation and migration, we first measured the levels of lactate in TNF-α-induced RA FLSs. We observed that lactate levels in the cell medium were increased after stimulation with TNF-α. However, this increase was suppressed by treatment with PFK15 or PFKFB3 siRNA (Figure 6A). To evaluate the relationship between lactate and proinflammatory cytokines and migration, lactate was added to the medium of cultured RA FLSs. The cells were treated with PFK15 for 3 h and then incubated with 10 mM lactic acid, which represents a lactate concentration present in the synovial fluid of RA patients (Haas *et al.,* 2015) and detected in a number of inflammatory sites (Young *et al.,* 2013). As shown in Figure 6B–D, the addition of lactate reversed the inhibitory effect of PFK15 or PFKFB3 siRNA on proinflammatory cytokines in TNF-α-stimulated RA FLSs. Lactate also reversed the inhibitory effect of PFKFB3 suppression on the migration of RA FLSs (Figure 6E).

Lactate is involved in PFKFB3-mediated activation of NF-κB and MAPK by RA FLS

We further investigated whether lactate was involved in the PFKFB3-mediated activation of NF-κB and MAPK pathways in RA FLSs. As shown in Figure 7A and B, the addition of lactate to PFK15-pretreated RA FLSs rescued the observed decrease in nuclear translocation of p65 as well as the phosphorylation of IKK and IκBα. The PFK15-induced decrease in p38, JNK and ERK activation was also reversed by the addition of lactate (Figure 7C). These data suggest that a decrease in lactate in PFKFB3-inhibited RA FLSs might be a major cause of NF-κB and MAPK inactivation.

PFK15 administration attenuates arthritis severity in mice with CIA

Given these observations in cultured RA FLSs, the *in vivo* effect of PFKFB3 inhibition by PFK15, on synovial inflammation and joint destruction in RA was evaluated in mice with CIA. In contrast to DMSO treatment, i.p. injection of PFK15 suppressed the increase in clinical score (Figure 8 A–B and Supporting Information Table S2 in the supplemental data). PFK15 treatment also decreased the

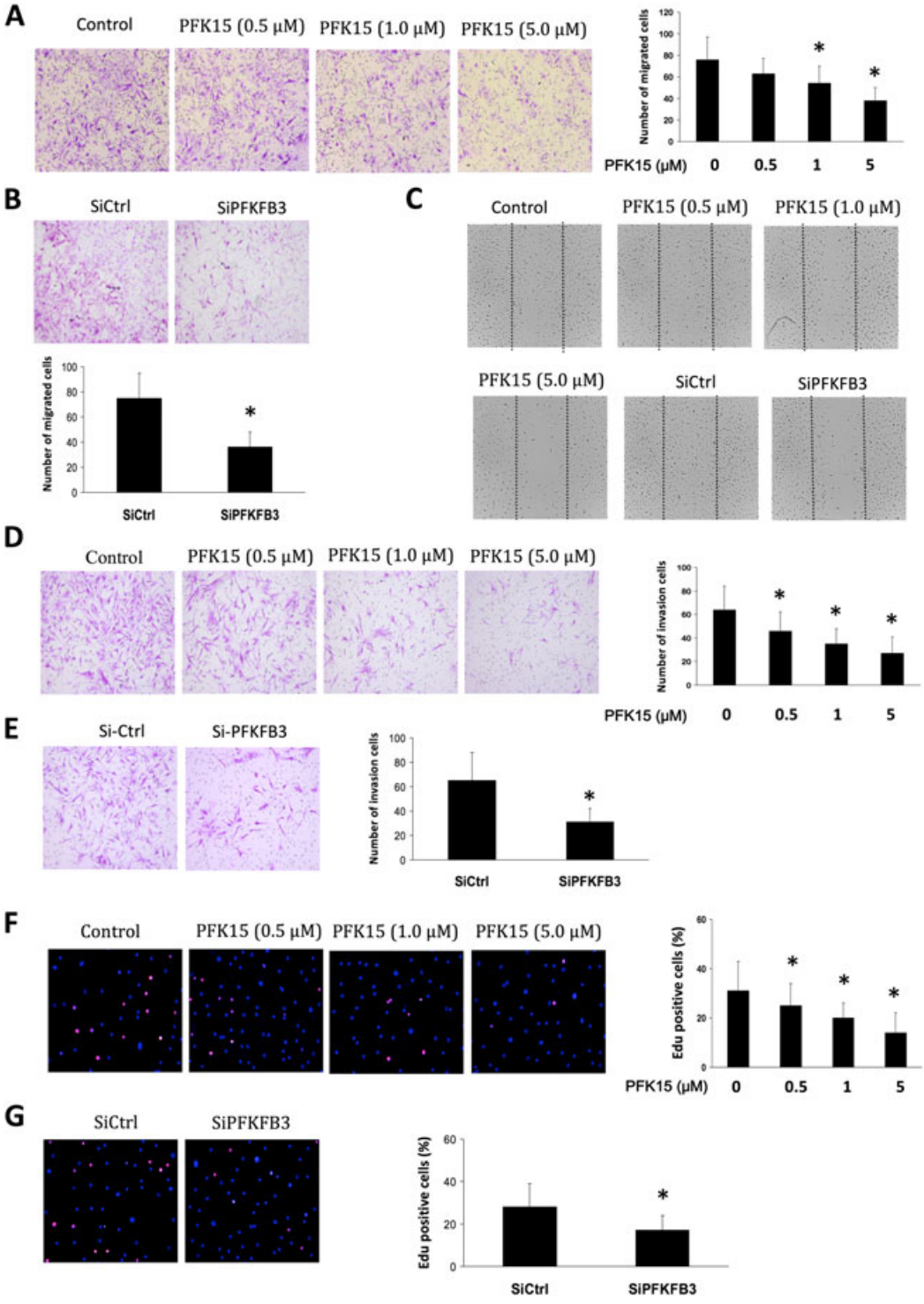

Figure 3

Effect of PFKFB3 inhibition on the migration, invasion and proliferation of RA FLSs. RA FLSs were pretreated with various concentrations of PFK15 for 4 h or transfected with PFKFB3 siRNA (Si-PFKFB3) or control siRNA (Si-Ctrl). (A–B) Migration was assayed in a Boyden chamber. The results show the means ± SEM for samples from eight different RA patients. The migrated FLSs were stained violet using a Diff-Quick kit [left (A) or upper (B) panel, original magnification 200×]. (C) Effect of PFKFB3 inhibition on the migration of RA FLSs after wounding. The images are representative of experiments from five different RA patients (original magnification 100×). (D–E) Effect of PFKFB3 inhibition on the invasion of RA FLSs. The results show the means ± SEM in samples from eight different RA patients. The migrated FLSs were stained violet using a Diff-Quick kit (left panel, original magnification 200×). (F–G) RA FLSs were incubated with or without PFK15 for 48 h. Cell proliferation was determined using the EdU assay. The data are presented as the means ± SEM of five independent experiments from five different RA patients (right panel). *$P < 0.05$, significantly different from control or Si-Ctrl.

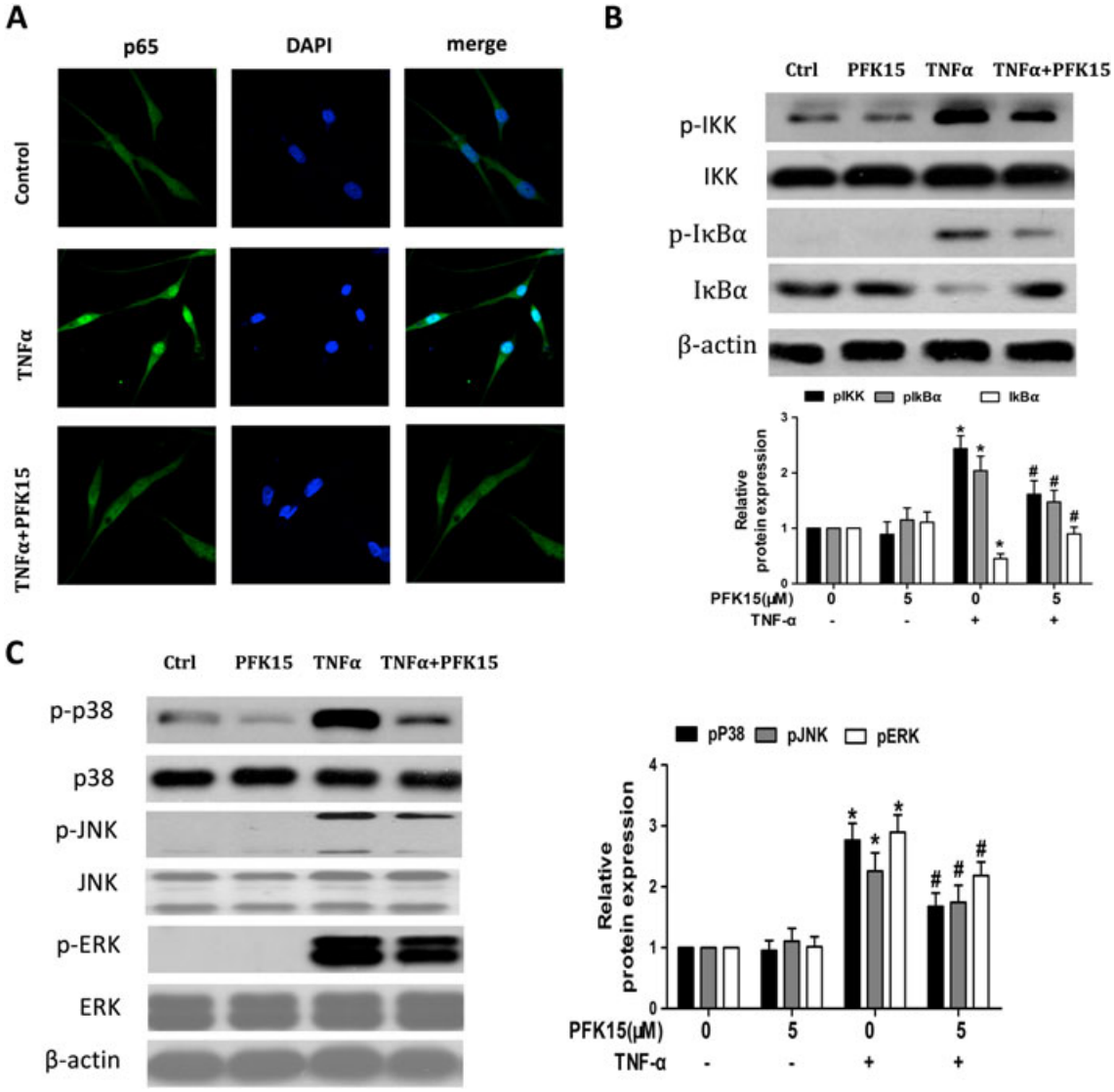

Figure 4

Role of PFKFB3 in regulating activation of the NF-κB and MAPK pathways. RA FLSs pretreated with the PFKFB3 inhibitor PFK15 (5 μM) for 4 h were stimulated with TNF-α for 30 min. (A) Effect of PFK15 on the nuclear translocation of NF-κB p65. Representative laser confocal microcopy images showing the effect of PFK15 on TNFα-induced translocation of p65 (green stain) from three independent experiments. (B) Effect of PFK15 on IKK and IκBα phosphorylation. The lower panel shows a densitometric analysis of a Western blot from five independent experiments. (C) Effect of PFK15 on the phosphorylation of p38, JNK and ERK. The right panel shows a densitometric analysis of an immunoblot from five independent experiments. *$P < 0.05$, significantly different from control (Ctrl); $^{\#}$ $P < 0.05$, significantly different from TNF-α alone.

inflammatory cell infiltrate and synovial hyperplasia along with the pannus invasion into calcified cartilage and bone (Figure 8C). We further observed that the serum levels and synovial expression of IL-6 were decreased in PFK15-treated CIA mice compared with those in DMSO-treated CIA mice (Figure 8D and E).

No significant gain in body weight was observed between the PFK15 and DMSO groups over the course of the experiment. We found no significant changes in renal (serum Cr levels), liver (ALT and AST levels) or serum glucose parameters in mice treated with PFK15 (data not shown). Furthermore, we also found no significant histopathological alterations in livers and kidneys removed from PFK15-treated mice compared with those of DMSO-treated mice (Figure 8F). These data demonstrate the safety of PFK15 treatment in mice with CIA.

Discussion

In the present study, we showed that PFKFB3 expression is increased in FLSs and synovial tissues derived from RA patients. We also demonstrated that PFKFB3 inhibition decreased the expression of proinflammatory cytokines, migration, invasion and proliferation of RA FLSs. The NF-κB and p38, JNK and ERK MAPK pathways were blocked by the

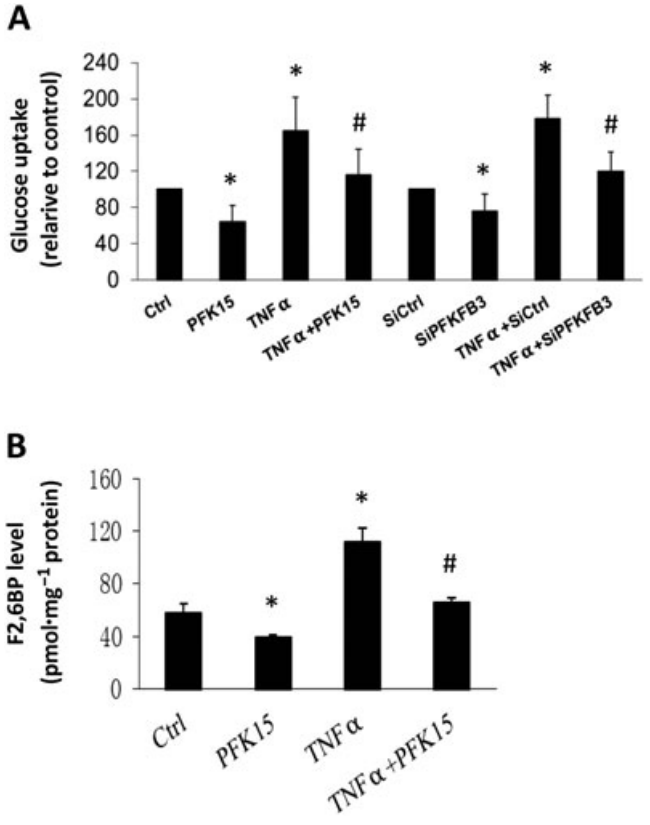

Figure 5

Effect of PFKFB3 inhibition on glucose uptake and intracellular levels of fructose-2,6-bisphosphate (F2,6BP) by RA FLSs. RA FLSs pretreated with the PFKFB3 inhibitor PFK15 (5 μM) for 4 h or transfected with PFKFB3 siRNA (SiPFKFB3) or control siRNA (SiCtrl) were stimulated with TNF-α for 24 h. Glucose uptake (A) was measured using a glucose uptake assay kit (colorimetric), and intracellular levels of F2,6BP (B) in RA FLSs were evaluated using a coupled enzyme assay. *$P < 0.05$, significantly different from control (Ctrl) or SiCtrl; $^{\#}P < 0.05$, significantly different from TNF-α.

PFKFB3 inhibitor. PFKFB3 inhibition also reduced glucose uptake and lactate secretion by RA FLSs. Treatment with PFK15 *in vivo* markedly reduced the severity of synovial hyperplasia, inflammatory cell infiltration and joint destruction in mice with CIA. Our findings strongly suggest an important role for the elevated PFKFB3 expression in the maintenance of the activated phenotype of FLSs in RA.

Pro-inflammatory cytokines and chemokines play a key role in synovial inflammation in RA. The detailed mechanisms underlying the regulation of the elevated production of a series of pro-inflammatory cytokines in RA remain unclear. Recent studies have shown that glycolytic inhibitors reduce proinflammatory cytokine expression in RA FLSs (Biniecka *et al.,* 2016; Garcia-Carbonell *et al.,* 2016). In this study, we demonstrated increased expression of PFKFB3 in FLSs and synovial tissues from RA patients compared with the levels in OA FLSs, and PFKFB3 inhibition decreased the expression of proinflammatory cytokines and chemokines in RA FLSs. These *in vitro* results were supported by *in vivo* experiments, showing that PFK15 attenuated synovial inflammation and joint destruction in mice with CIA. Thus, our findings further support the notion that increased synovial glycolytic metabolism contributes to joint inflammation in RA.

The migration of FLSs to cartilage and bone is a critical process for joint destruction in RA. FLSs can destroy cartilage and activate osteoclasts (Gravallese *et al.,* 2000; Müller-Ladner *et al.,* 2005). Accumulating evidence suggests the potential importance of FLS-mediated joint destruction in RA. However, no effective treatments have been found to directly target FLS-mediated joint destruction. Clarifying the detailed mechanisms by which the aggressive capacity of FLSs is controlled could ultimately result in new therapies for RA.

Recent studies demonstrated an association of PFKFB3 with the migration and growth of breast cancer (Ge *et al.,* 2015), osteosarcoma cells (Du *et al.,* 2015) and bladder cancer (Sun *et al.,* 2016). The role of PFKFB3 in tumour cells supports a relationship between PFKFB3 and the aggressive nature of RA FLSs. In the present study, we demonstrated that inhibition of PFKFB3 by the specific inhibitor PFK15 or siRNA significantly reduced migration based on wound-healing and chemotaxis assays. Similar findings were obtained for the regulation of the invasive behaviour of RA FLSs through Matrigel-coated Transwell membranes. These data suggest that overexpression of PFKFB3 may contribute to the aberrant aggressive behaviour of RA FLSs. Consistent with our results, PFKFB3 inhibition also reduced the directional migration of endothelial cells (De Bock *et al.,* 2013; Schoors *et al.,* 2014).

Deletion of the *Pfkfb3* gene reduced cancer cell glucose metabolism and tumour growth, making this enzyme a promising target for anti-cancer therapy (Telang *et al.,* 2006). More interestingly, heterozygous genomic deletion of PFKFB3 resulted in a 50% reduction in PFKFB3 protein expression in all examined cell types, but it did not cause a reduction in birth weight, litter size, development or ageing (Chesney *et al.,* 2005). In addition, the administration of PFK15 *in vivo* did not result in toxicity in mice (Clem *et al.,* 2008; Clem *et al.,* 2013). These findings suggest good tolerance in mice of therapies that suppress PFKFB3. A recent report showed that inhibition of PFKFB3 attenuates the development of an established mouse model of psoriasis (Telang *et al.,* 2012). In this work, we demonstrated that i.p. administration of PFK15 ameliorated the severity of arthritis, including clinical scores, histopathological parameters of synovial inflammation and bone resorption and reduced serum levels and synovial expression of IL-6 in mice with CIA. Importantly, there were no significant changes in the body weight, serum glucose or renal or liver parameters in mice treated with PFK15 over the course of the experiment, supporting the safety of PFK15 treatment in CIA mice.

As a critical transcriptional factor in modulating the expression of a number of proinflammatory genes, NF-κB is considered a key signalling molecule in the control of synovial inflammation, hyperplasia and matrix degeneration (Miagkov *et al.,* 1998; Tak *et al.,* 2001; Hammaker *et al.,* 2003; Thalhamer *et al.,* 2008). To explore the mechanisms by which PFKFB3 regulates synovial inflammatory responses, we evaluated the effect of PFKFB3 inhibition on NF-κB activation. We observed that PFK15 suppressed TNF-α-induced phosphorylation of IKK and IκBα, as well as the

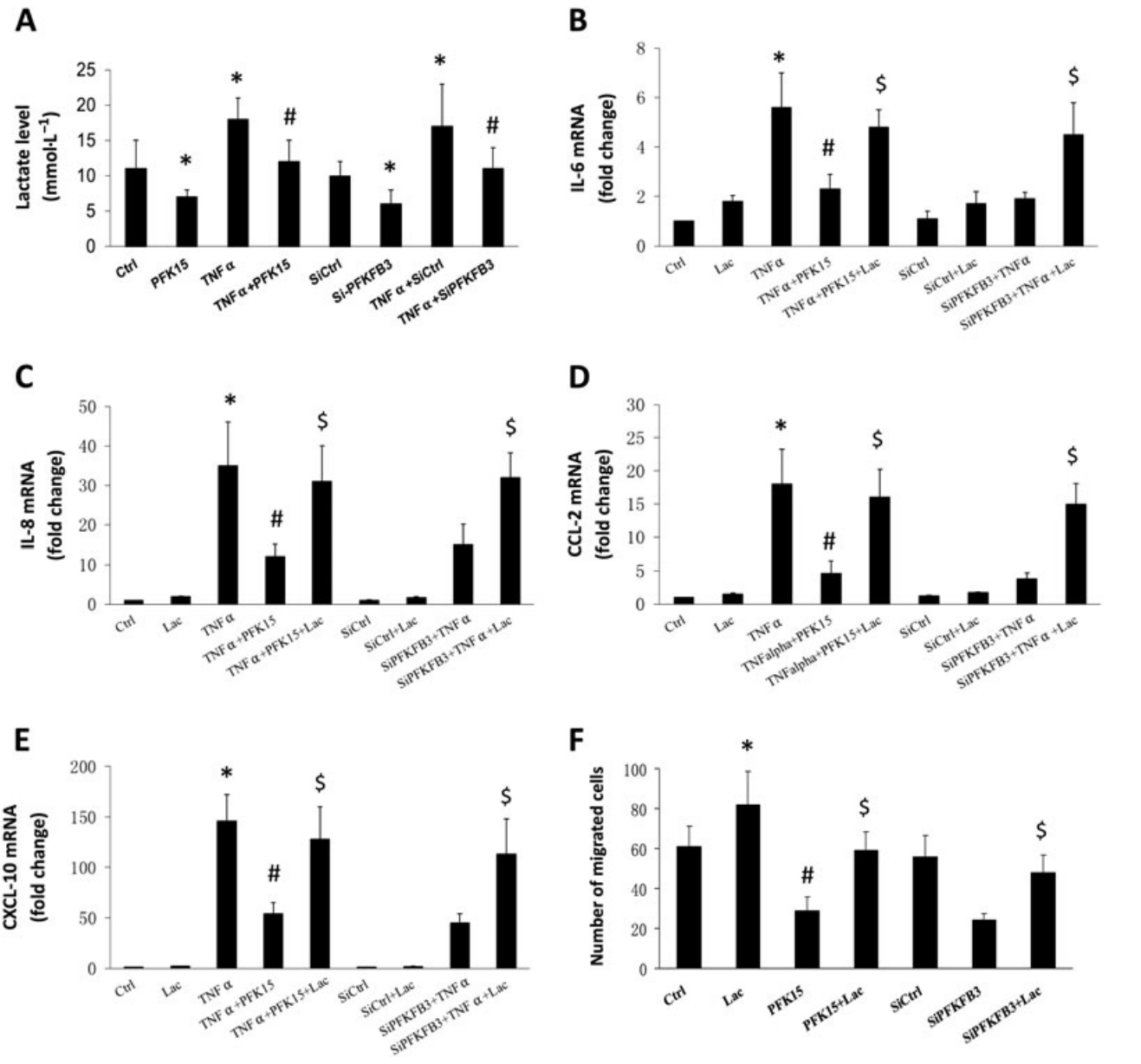

Figure 6

Role of lactate in regulating PFKFB3-mediated inflammation and migration of RA FLSs. (A) Effect of PFKFB3 inhibition on lactate secretion. RA FLSs pretreated with PFKFB3 inhibitor PFK15 (5 μM) for 4 h or transfected with PFKFB3 siRNA (SiPFKFB3) or control siRNA (SiCtrl) were stimulated with TNF-α for 24 h. Lactate concentrations in the supernatants of cultured RA FLSs were evaluated using a lactate oxidase-based assay. (B–D) RA FLSs were pretreated with DMSO (as the Ctrl) or PFK15 for 4 h or were transfected with specific PFKFB3 siRNA (SiPFKFB3) or control siRNA (SiCtrl) and then stimulated with or without TNF-α (10 ng·mL^{-1}) for 24 h. Lactic acid (10 mM) was added for 6 h before harvesting the cells. The expression levels of IL-6 (B), IL-8 (C), CCL-2 (D) and CXCL-10 (E) were measured by real-time qPCR. The data are representative of five independent experiments (means ± SEM). *$P < 0.05$, significantly different from Ctrl or SiCtrl; $^{\#}P < 0.05$, significantly different from TNF-α alone; $^{\$}P < 0.05$, significantly different from TNF-α + PFK15.

translocation of nuclear NF-κB, suggesting that PFKFB3 regulates the NF-κB pathway by interfering with early cytoplasmic IKK signalling.

MAPKs also play important roles in transducing synovial inflammation and joint destruction, and they are considered critical molecular targets for therapeutic intervention in RA (Thalhamer *et al.,* 2008). The p38 MAPK isoforms are involved in regulating many of the cellular biological processes, particularly synovial inflammatory cytokine production, which contributes to the pathogenesis of RA (Korb *et al.,* 2006; Schett *et al.,* 2008). The JNK MAPK appears to play a major role in modulating collagenase production and invasion by RA FLSs (Han *et al.,* 2001; Fu *et al.,* 2012). The ERK MAPK participates in regulating the synthesis of IL-6, IL-12, IL-23 and TNF-α and in promoting pannus formation (Goodridge *et al.,* 2003). In this study,

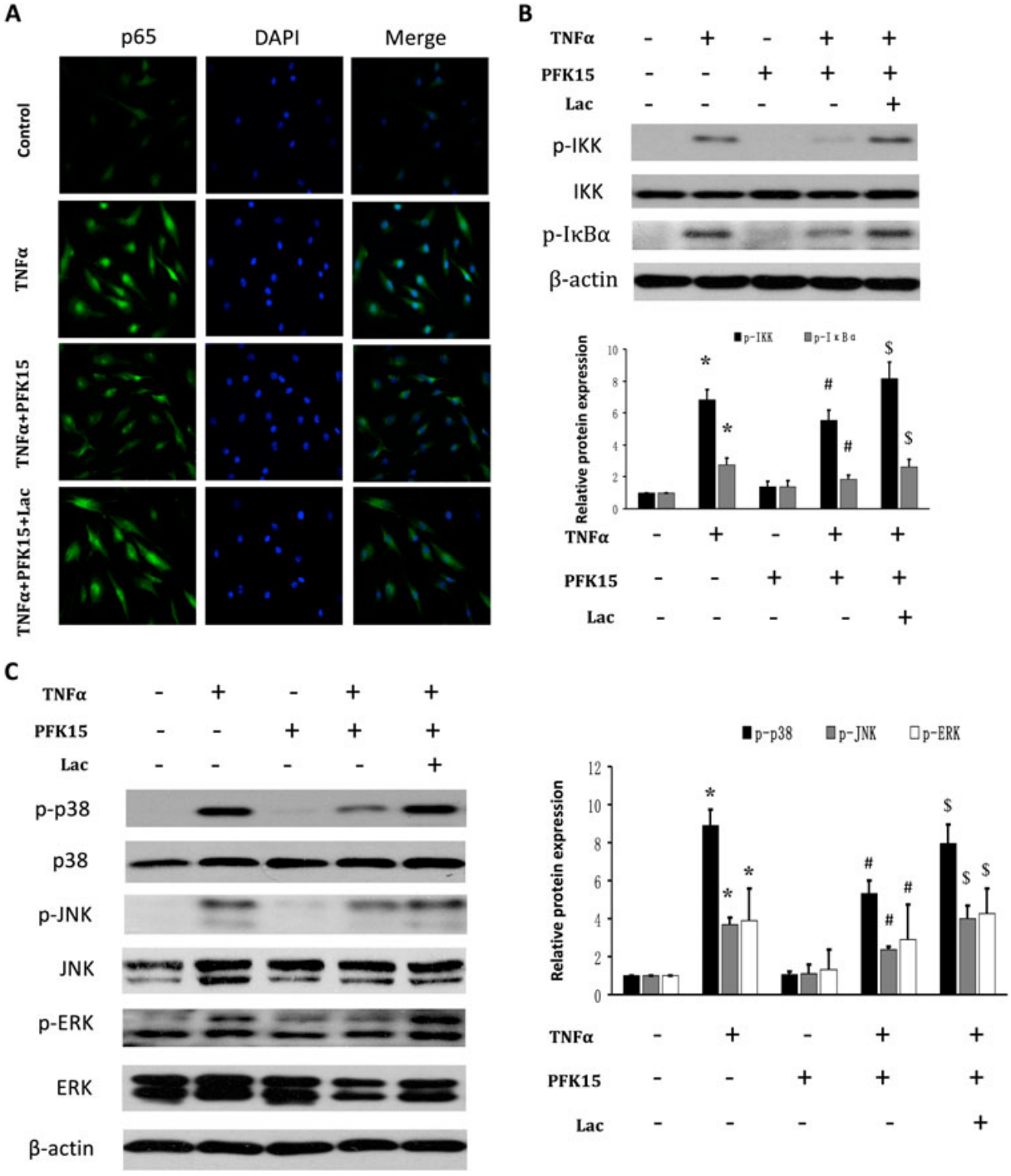

Figure 7

Involvement of lactate in the PFKFB3-mediated activation of NF-κB and MAPK pathways by RA FLSs. RA FLSs were treated with or without the PFKFB3 inhibitor PFK15 (5 μM) for 4 h and then incubated with or without lactic acid (Lac, 10 mM) for 6 h. The cells were stimulated with TNF-α for 30 min before harvesting. (A) Effect of lactate treatment on nuclear translocation of NF-κB p65. Representative laser confocal microcopy images showing the effect of lactate on TNFα-induced translocation of p65 (green stain) from five independent experiments. (B) Effect of lactate on IKK and IκBα phosphorylation. The lower panel shows a densitometric analysis of Western blotting from five independent experiments. (C) Effect of lactate on the phosphorylation of p38, JNK and ERK. The right panel shows a densitometric analysis of immunoblot analyses from five independent experiments. *$P < 0.05$ versus control (Ctrl); $^{\#}P < 0.05$, significantly different from TNF-α alone; $^{\$}P < 0.05$, significantly different from TNF-α + PFK15.

we found, for the first time, that PFKFB3 inhibition suppressed the phosphorylation of p38, JNK and ERK by TNF-α-stimulated RA FLSs. Collectively, our findings indicate that glycolytic metabolism contributes to synovial inflammation and invasiveness, at least in part by regulating the NF-κB and p38/JNK/ERK pathways.

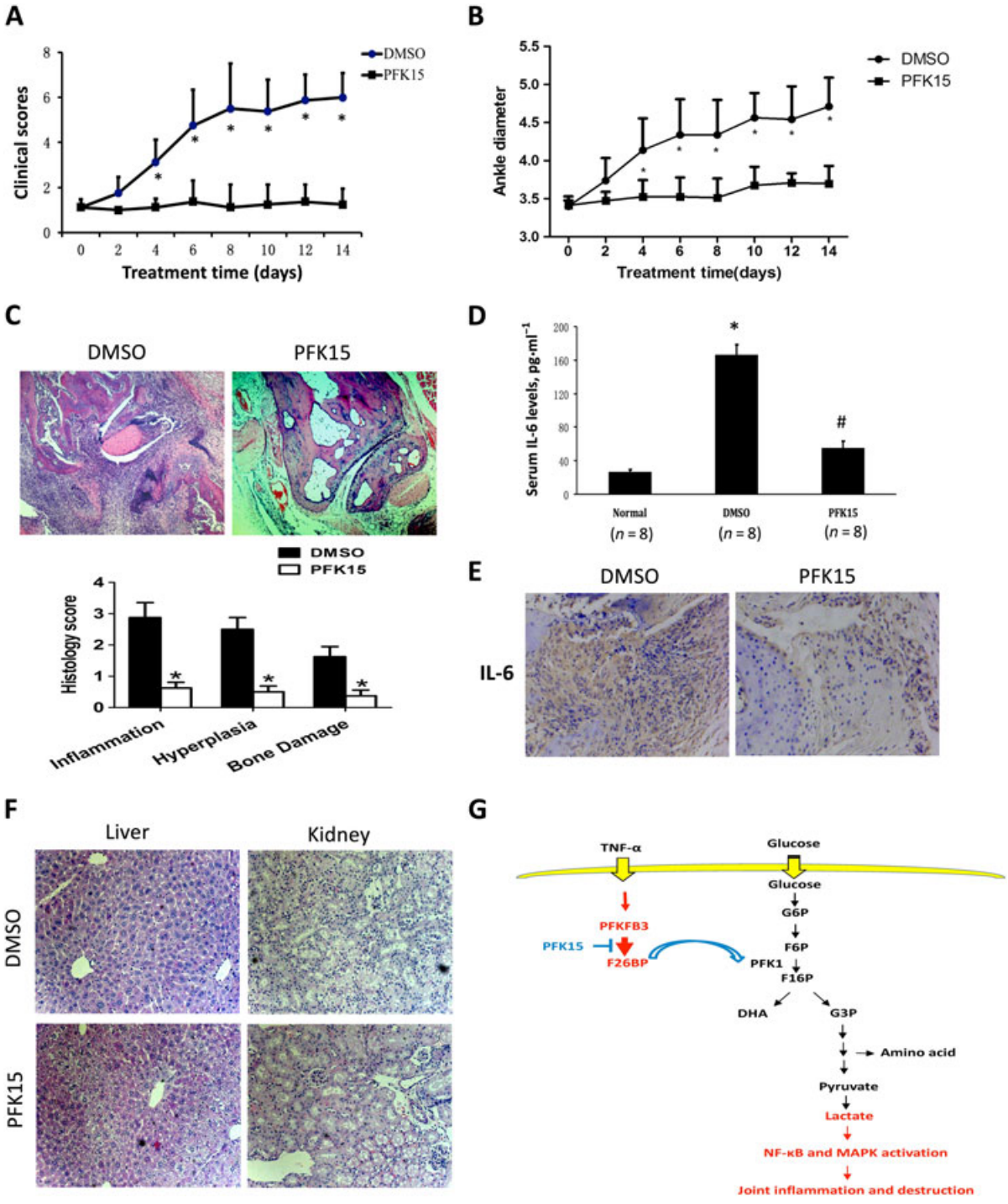

Figure 8

Attenuation of severity of arthritis in mice with CIA by the PFKFB3 inhibitor PFK15. (A–B) Effect of PFK15 on the clinical score (A) and ankle diameter (B) in mice with CIA. The values in A and B are the means ± SEM of eight mice injected i.p. with PFK15 (25 mg·kg^{-1}, every other day) and eight mice treated with DMSO. (C) Histological findings. The specimens from the removed arthritic paws were stained with H&E (original magnification 100×). The lower panel shows the scores (means ± SEM) for synovial inflammation, hyperplasia and bone loss. *$P < 0.05$, significantly different from DMSO. (D) Effect of PFK15 on serum levels of IL-6 in CIA mice. The levels of IL-6 were measured by ELISA. The values are the means ± SEM. *$P < 0.05$, significantly different from normal control; $^{\#}P < 0.05$, significantly different from DMSO. (E) Effect of PFK15 on the expression of IL-6 in synovial tissue from mice with CIA. IL-6 expression was measured by immunohistochemical staining. Representative images of IL-6 expression in synovial tissues are shown for DMSO-treated (n = 5) and PFK15-treated (n = 5) mice (original magnification 200×). (F) Effect of PFK15 on the liver and kidney of CIA mice. Photomicrographs show the histopathology of the liver and kidney from DMSO- or PFK15-treated mice. Original magnification 100×. (G) Diagram of the proposed role of PFKFB3 in regulating synovial inflammation and joint destruction in RA.

Because of a high level of glycolysis, activated RA FLSs produce a substantial amount of lactate (Yang *et al.,* 2015; Biniecka *et al.,* 2016). Previous studies have indicated that lactate functions as an important molecule in the regulation of intracellular signalling pathways under physiological and pathological conditions. For example, lactate is involved in angiogenesis by activating the endothelial PI3K/Akt pathway (Ruan and Kazlauskas, 2013). Lactate, which is derived from tumour cells, plays a key role in signalling that modulates the polarization of tumour-associated macrophages (Colegio *et al.,* 2014). Lactic acid also induces endothelial tube formation *via* NF-κB activation (Vegran *et al.,* 2011). Moreover, lactate-induced Akt phosphorylation has been reported to participate in PFKFB3-driven endothelial angiogenesis (Xu *et al.,* 2014). Thus, to determine the mechanisms linking PFKFB3 inhibition to the inhibition of NF-κB and MAPK activity, we examined whether lactate could mediate the role of PFKFB3 in regulating the activation of NF-κB and MAPK signals in RA FLSs. We found that PFKFB3 inhibition decreased the levels of lactate in RA FLSs. The addition of lactate to RA FLSs reversed the inhibitory effect of PFKFB3 suppression on NF-κB and MAPK signalling activation. Moreover, the impaired invasion and proinflammatory cytokine expression were reversed by exogenous lactate. Therefore, as summarized in Figure 8G, PFKFB3 inhibition caused a low level of glycolysis and lactate, which resulted in a decrease in NF-κB and MAPK signalling activation, as well as the prevention of synovial inflammation and joint destruction in RA. However, the mechanisms underlying lactate-mediated induction of proinflammatory cytokine expression and aggressiveness in RA FLSs remain unclear and require further investigation. In addition, it is well established that F-2,6-BP, which is produced by PFKFB3, plays a critical role in regulating glycolysis in the cytoplasm (Okar *et al.,* 1999; Okar *et al.,* 2001; Smith *et al.,* 2007; Telang *et al.,* 2012). However, our findings indicate that PFKFB3 protein is predominantly localized in the nucleus. We suspect that both non-mutually exclusive mechanisms might provide explanations for this controversial issue. One possibility is that PFKFB3 protein shuttles out of the nucleus to the cytoplasm. However, this phenomenon seems unlikely because we did not observe TNF-α-induced translocation of PFKFB3 from the nucleus to the cytoplasm (Supporting Information Fig. S2 in the supplemental data). The other model is the subcellular compartmentalization of F-2,6-BP such that nuclear F-2,6-BP might be transferred to the cytoplasm under stimulation because of an established concentration gradient of F-2,6-BP between the nucleus and cytoplasm. Consequently, a relative increase in F-2,6-BP in the cytoplasm might result in the induction of glycolysis. Indeed, it has been reported that nuclear-to-cytosolic gradients of small molecules, such as calcium ions, are preserved in mitogen-stimulated hepatocytes (Waybill *et al.,* 1991).

In conclusion, our observations showed that the inhibition of PFKFB3 kinase activity reduced the activation and aggressive capacity of RA FLSs *in vitro* and induced suppression of experimental arthritis *in vivo*, which suggests that targeting PFKFB3 may be a novel therapeutic strategy for inflammatory arthritis.

Acknowledgements

The authors would like to thank Jinjin Fan for her technical assistance. This work is supported by grants from National Natural Science Foundation of China (Grant number 81373182, U1401222, 81671591, 8150060222), Guangdong Natural Science Foundation (Grant number S2011020002358, S2013010015363) and Guangdong Project of Science and Technology (Grant number 2016A020215043).

Author contributions

Y.Z., S.Z. and M.H. performed the research, designed the research study, analysed the data and supervised the study. Q.Q. and Y.X. designed the research study, analysed the data, provided critical discussions and approved the version to be published. M.S. performed the research and analysed the data. Z.Z., L.L. and X.Y. provided critical discussions and approved the version to be published. H.X. supervised the study, analysed the data, provided critical discussions, wrote the paper and approved the version to be published.

Conflict of interest

The authors declare no conflicts of interest.

Declaration of transparency and scientific rigour

This Declaration acknowledges that this paper adheres to the principles for transparent reporting and scientific rigour of preclinical research recommended by funding agencies, publishers and other organisations engaged with supporting research.

References

Alexander SPH, Fabbro D, Kelly E, Marrion N, Peters JA, Benson HE *et al.* (2015). The Concise Guide to PHARMACOLOGY 2015/16: Enzymes. Br J Pharmacol 172: 6024–6109.

Arnett FC, Edworthy SM, Bloch DA, McShane DJ, Fries JF, Cooper NS *et al.* (1988). The American Rheumatism Association 1987 revised criteria for the classification of rheumatoid arthritis. Arthritis Rheum 31: 315–324.

Biniecka M, Canavan M, McGarry T, Gao W, McCormick J, Cregan S *et al.* (2016). Dysregulated bioenergetics: a key regulator of joint inflammation. Ann Rheum Dis published on 24 Mar 2016. doi:10.1136/annrheumdis-2015-208476.

Bottini N, Firestein GS (2013). Duality of fibroblast-like synoviocytes in RA: passive responders and imprinted aggressors [review]. Nat Rev Rheumatol 9: 24–33.

Chang SK, Gu Z, Brenner MB (2010). Fibroblast-like synoviocytes in inflammatory arthritis pathology: the emerging role of cadherin-11. Immunol Rev 233: 256–266.

Chesney J, Telang S, Yalcin A, Clem A, Wallis N, Bucala R (2005). Targeted disruption of inducible 6-phosphofructo-2-kinase results in embryonic lethality. Biochem Biophys Res Commun 331: 139–146.

Choy E (2012). Understanding the dynamics: pathways involved in the pathogenesis of rheumatoid arthritis [review]. Rheumatology (Oxford) 51: v3–v11.

Clem B, Telang S, Clem A, Yalcin A, Meier J, Simmons A *et al.* (2008). Small-molecule inhibition of 6-phosphofructo-2-kinase activity suppresses glycolytic flux and tumor growth. Mol Cancer Ther 7: 110–120.

Clem BF, O'Neal J, Tapolsky G, Clem AL, Imbert-Fernandez Y, Kerr DA 2nd *et al.* (2013). Targeting 6-phosphofructo-2-kinase (PFKFB3) as a therapeutic strategy against cancer. Mol Cancer Ther 12: 1461–1470.

Colegio OR, Chu NQ, Szabo AL, Chu T, Rhebergen AM *et al.* (2014). Functional polarization of tumor associated macrophages by tumor-derived lactic acid. Nature 513: 559–563.

Curtis MJ, Bond RA, Spina D, Ahluwalia A, Alexander SP, Giembycz MA *et al.* (2015). Experimental design and analysis and their reporting: new guidance for publication in BJP. Br J Pharmacol 172: 3461–3471.

De Bock K, Georgiadou M, Schoors S *et al.* (2013). Role of PFKFB3-driven glycolysis in vessel sprouting. Cell 154: 651–663.

Du JY, Wang LF, Wang Q, Yu LD (2015). miR-26b inhibits proliferation, migration, invasion and apoptosis induction via the downregulation of 6-phosphofructo-2-kinase/fructose-2, 6-bisphosphatase-3 driven glycolysis in osteosarcoma cells. Oncol Rep 33: 1890–1898.

Fu D, Yang Y, Xiao Y, Lin H, Ye Y, Zhan Z *et al.* (2012). Role of p21-activated kinase 1 in regulating the migration and invasion of fibroblast-like synoviocytes from rheumatoid arthritis patients. Rheumatology 51: 1170–1180.

Garcia-Carbonell R, Divakaruni AS, Lodi A, Vicente-Suarez I, Saha A, Cheroutre H *et al.* (2016). Critical role of fibroblast-like synoviocytes glycolytic metabolism in rheumatoid arthritis. Arthritis Rheumatol 68: 1614–1626.

Ge X, Lyu P, Cao Z, Li L, Li J, Wang Y*et al.* (2015). Overexpression of miR-206 suppresses glycolysis, proliferation and migration in breast cancer cells via PFKFB3 targeting. Biochem Biophys Res Commun 463: 1115–1121.

Goodridge HS, Harnett W, Liew FY, Harnett MM (2003). Differential regulation of interleukin-12 p40 and p35 induction via Erk mitogen-activated protein kinase-dependent and -independent mechanisms and the implications for bioactive IL-12 and IL-23 responses. Immunology 109: 415–425.

Gravallese EM, Manning C, Tsay A, Naito A, Pan C, Amento E *et al.* (2000). Synovial tissue in rheumatoid arthritis is a source of osteoclast differentiation factor. Arthritis Rheum 43: 250–258.

Haas R, Smith J, Rocher-Ros V, Nadkarni S, Montero-Melendez T, D'Acquisto F *et al.* (2015). Lactate regulates metabolic and pro-inflammatory circuits in control of T cell migration and effector functions. PLoS Biol 13: e1002202.

Hammaker D, Sweeney S, Firestein GS (2003). Signal transduction networks in rheumatoid arthritis. Ann Rheum Dis 62: 1186–1189.

Han Z, Boyle DL, Chang L, Bennett B, Karin M, Yang L *et al.* (2001). c-Jun N-terminal kinase is required for metalloproteinase expression and jointdestruction in inflammatory arthritis. J Clin Invest 108: 73–81.

Kilkenny C, Browne W, Cuthill IC, Emerson M, Altman DG (2010). Animal research: reporting in vivo experiments: the ARRIVE guidelines. Br J Pharmacol 160: 1577–1579.

Korb A, Tohidast-Akrad M, Cetin E, Axmann R, Smolen J, Schett G (2006). Differential tissue expression and activation of p38 MAPK alpha, beta, gamma, and delta isoforms in rheumatoid arthritis. Arthritis Rheum 54: 2745–2756.

Leung BP, Sattar N, Crilly A, Prach M, McCarey DW, Payne H *et al.* (2003). A novel anti-inflammatory role for simvastatin in inflammatory arthritis. J Immunol 170: 1524–1530.

Lunt SY, Vander Heiden MG (2011). Aerobic glycolysis: meeting the metabolic requirements of cell proliferation. Annu Rev Cell Dev Biol 27: 441–464.

McGrath JC, Lilley E (2015). Implementing guidelines on reporting research using animals (ARRIVE etc.): new requirements for publication in BJP. Br J Pharmacol 172: 3189–3193.

Miagkov AV, Kovalenko DV, Brown CE, Didsbury JR, Cogswell JP, Stimpson SA *et al.* (1998). NF-kappaB activation provides the potential link between inflammation and hyperplasia in the arthritic joint. Proc Natl Acad Sci U S A 95: 13859–13864.

Müller-Ladner U, Pap T, Gay RE, Neidhart M, Gay S (2005). Mechanisms of disease: the molecular and cellular basis of joint destruction in rheumatoid arthritis. Nat Clin Pract Rheumatol 1: 102–110.

Okar DA, Live DH, Kirby TL, Karschnia EJ, von Weymarn LB, Armitage IM *et al.* (1999). The roles of Glu-327 and His-446 in the bisphosphatase reaction of rat liver 6-phosphofructo-2-kinase/ fructose-2,6-bisphosphatase probed by NMR spectroscopic and mutational analyses of the enzyme in the transient phosphohistidine intermediate complex. Biochemistry 38: 4471–4479.

Okar DA, Manzano A, Navarro-Sabatè A, Riera L, Bartrons R, Lange AJ (2001). PFK-2/FBPase-2: maker and breaker of the essential biofactor fructose-2,6-bisphosphate. Trends Biochem Sci 26: 30–35.

Rider MH, Bertrand L, Vertommen D, Michels PA, Rousseau GG, Hue L (2004). 6-phosphofructo-2-kinase/fructose-2,6-bisphosphatase: head-to-head with a bifunctional enzyme that controls glycolysis. Biochem J 381: 561–579.

Ruan GX, Kazlauskas A (2013). Lactate engages receptor tyrosine kinases axl, tie2, and vascular endothelial growth factor receptor 2 to activate phosphoinositide 3-kinase/akt and promote angiogenesis. J Biol Chem 288: 21161–21172.

Schett G, Zwerina J, Firestein G (2008). The p38 mitogen-activated protein kinase (MAPK) pathway in rheumatoid arthritis. Ann Rheum Dis 67: 909–916.

Schoors S, De Bock K, Cantelmo AR, Georgiadou M, Ghesquière B, Cauwenberghs S *et al.* (2014). Partial and transient reduction of glycolysis by PFKFB3 blockade reduces pathological angiogenesis. Cell Metab 19: 37–48.

Schulze A, Harris AL (2012). How cancer metabolism is tuned for proliferation and vulnerable to disruption [review]. Nature 491: 364–373.

Smith WE, Langer S, Wu C, Baltrusch S, Okar DA (2007). Molecular coordination of hepatic glucose metabolism by the 6-phosphofructo-2-kinase/ fructose-2,6-bisphosphatase:glucokinase complex. Mol Endocrinol 21: 1478–1487.

Southan C, Sharman JL, Benson HE, Faccenda E, Pawson AJ, Alexander SPH *et al.* (2016). The IUPHAR/BPS Guide to PHARMACOLOGY in 2016: towards curated quantitative

interactions between 1300 protein targets and 6000 ligands. Nucl Acids Res 44 (Database Issue): D1054–D1068.

Sun CM, Xiong DB, Yan Y, Geng J, Liu M, Yao XD (2016). Genetic alteration in phosphofructokinase family promotes growth of muscle-invasive bladder cancer. Int J Biol Markers 31: e286–e293.

Tak PP, Gerlag DM, Aupperle KR, van de Geest DA, Overbeek M, Bennett BL *et al.* (2001). Inhibitor of nuclear factor κB is a key regulator of synovial inflammation. Arthritis Rheum 44: 1897–1907.

Telang S, Yalcin A, Clem AL, Bucala R, Lane AN, Eaton JW *et al.* (2006). Ras transformation requires metabolic control by 6-phosphofructo-2-kinase. Oncogene 25: 7225–7234.

Telang S, Clem BF, Klarer AC, Clem AL, Trent JO, Bucala R *et al.* (2012). Small molecule inhibition of 6-phosphofructo-2-kinase suppresses T cell activation. J Transl Med 10: 95. doi:10.1186/1479-5876-10-95.

Thalhamer T, McGrath MA, Harnett MM (2008). MAPKs and their relevance to arthritis and inflammation. Rheumatology (Oxford) 47: 409–414.

Tolboom TC, van der Helm-Van Mil AH, Nelissen RG, Breedveld FC, Toes RE, Huizinga TW (2005). Invasiveness of fibroblast-like synoviocytes is an individual patient characterize associated with the rate of joint destruction in patients with rheumatoid arthritis. Arthritis Rheum 52: 1999–2002.

Turner JD, Filer A (2015). The role of the synovial fibroblast in rheumatoid arthritis pathogenesis. Curr Opin Rheumatol 27: 175–182.

Van Schaftingen E, Hue EL, Hers HG (1980). Fructose 2, 6-bisphosphate, the probably structure of the glucose- and glucagon-sensitive stimulator of phosphofructokinase. Biochem J 192: 897–901.

Van Schaftingen E, Lederer B, Bartrons R, Hers HG (1982). A kinetic study of pyrophosphate: fructose-6-phosphate phosphotransferase from potato tubers. Application to a microassay of fructose 2, 6-bisphosphate. Eur J Biochem 129: 191–195.

Vegran F, Boidot R, Michiels C, Sonveaux P, Feron O (2011). Lactate influx through the endothelial cell monocarboxylate transporter MCT1 supports an NF-κB/IL-8 pathway that drives tumor angiogenesis. Cancer Res 1: 2550–2560.

Waybill MM, Yelamarty RV, Zhang YL, Scaduto RC Jr, LaNoue KF, Hsu CJ *et al.* (1991). Nuclear calcium gradients in cultured rat hepatocytes. Am J Physiol Endocrinol Metab 261: E49–E57.

Xu H, He Y, Yang Y, Liang L, Zhan Z, Ye Y*et al.* (2007). Anti-malarial agent artesunate inhibits TNFα-induced production of proinflammatory cytokines via inhibition of NF-κB and PI3 kinase/Akt signal pathway in human rheumatoid arthritis fibroblast-like synoviocytes. Rheumatology (Oxford) 46: 920–926.

Xu Y, An X, Guo X, Habtetsion TG, Wang Y, Xu X *et al.* (2014). Endothelial PFKFB3 plays a critical role in angiogenesis. Arterioscler Thromb Vasc Biol 34: 1231–1239.

Yang XY, Zheng KD, Lin K, Zheng G, Zou H, Wang JM *et al.* (2015). Energy metabolism disorder as a contributing factor of rheumatoid arthritis: a comparative proteomic and metabolomic study. PLoS One 10: e0132695.

Young SP, Kapoor SR, Viant MR, Byrne JJ, Filer A, Buckley CD *et al.* (2013). The impact of inflammation on metabolomics profiles in patients with arthritis. Arthritis Rheum 65: 2015–2023.

Supporting Information

Additional Supporting Information may be found online in the supporting information tab for this article:

http://doi.org/10.1111/bph.13762

Figure S1 Targeted depletion of PFKFB3 in RA FLSs. RA FLSs were transfected with siRNA for the PFKFB3 oligonucleotide (Si-PFKFB3), the control (Si-Ctrl) or GAPDH (as a positive control, Si-GAPDH). After 72 h of transfection, the cells were lysed. Gene expression of PFKFB3 (A) and GAPDH (B) was determined by real-time qPCR, and the presented mRNA expression values represent the means ± SEM from 5 independent experiments. PFKFB3 protein expression (C) was assessed by Western blot analysis. Semi-quantitative densitometry of PFKFB3 expression is shown in panel D from 5 independent experiments (means ± SEM). *$P < 0.05$ versus Si-Ctrl.

Figure S2 Effect of TNF-α on the translocation of PFKFB3 in RA FLSs. Cells were stimulated with TNF-α (10 ng/mL) for 12 h. Immunofluorescence staining was used to evaluate the expression of PFKFB3. Nuclei were stained with 4′-6-diamidono-2- phenylindole dihydrochloride (DAPI), and F-actin was stained with phalloidin. Representative laser confocal microscopy images showing the staining of PFKFB3 from 5 independent experiments. Original magnification 400 ×.

Table S1 The sequences of PFKFB3 siRNA oligonucleotides.

Table S2 Clinical scores for individual mice with collagen-induced arthritis.